Smart Structures and Systems, *Vol. 32*, *No. 3* (*2023*) *153-166*
https://doi.org/10.12989/sss.2023.32.3.153

Damage identification in a wrought iron railway bridge using the inverse analysis of the static stress response under rail traffic loading

Sidali Iglouli*[1,2], Nadir Boumechra [1,2a] and Karim Hamdaoui [1,2b]

[1] *Civil Engineering Department*, *Faculty of Technology*, *Tlemcen University*, *BP230-13000 Tlemcen*, *Algeria*
[2] *EOLE Laboratory*, *Faculty of Technology*, *Tlemcen University*, *BP 230-13000 Tlemcen*, *Algeria*

(*Received December 20*, *2022*, *Revised February 16*, *2023*, *Accepted March 3*, *2023*)

Abstract. Health monitoring of civil infrastructures, in particular, old bridges that are still in service, has become more than necessary, given the risk that a possible degradation or failure of these infrastructures can induce on the safety of users in addition to the resulting commercial and economic impact. Bridge integrity assessment has attracted significant research efforts over the past forty years with the aim of developing new damage identification methods applicable to real structures. The bridge of Ouled Mimoun (Tlemcen, Algeria) is one of the oldest railway structure in the country. It was built in 1889. This bridge, which is too low with respect to the level of the road, has suffered multiple shocks from various machines that caused considerable damage to its central part. The present work aims to analyze the stability of this bridge by identifying damages and evaluating the damage rate in different parts of the structure on the basis of a finite element model. The applied method is based on an inverse analysis of the normal stress responses that were calculated from the corresponding recorded strains, during the passage of a real train, by means of a set of strain gauges placed on certain elements of the bridge. The results obtained from the inverse analysis made it possible to successfully locate areas that were really damaged and to estimate the damage rate. These results were also used to detect an excessive rigidity in certain elements due to the presence of plates, which were neglected in the numerical reference model. In the case of the continuous bridge monitoring, this developed method will be a very powerful tool as a smart health monitoring system, allowing engineers to take in time decisions in the event of bridge damage.

Keywords: damage identification; health monitoring; inverse analysis; railway bridge; static; strain; stress response

1. Introduction

Rail transport in Algeria has grown steadily since its inception in 1857. Rail traffic is expected to reach a capacity of 160 million passengers and 60 million tons of freight per year by 2025. In fact, the existing network extends over a distance of 4600 km and includes more than 2000 railway bridges of which about 20% have existed for more than a century (Boukezzi *et al*. 2021). These bridges represent the most sensitive sections because their eventual degradation or disruption can seriously affect the safety of travelers, and may have substantial commercial and economic repercussions.

Considering the problems of dilapidation, inefficiency of the standard visual inspection procedure, and the high costs of maintenance, repair and rehabilitation of railway bridges, it has become increasingly difficult to meet future requirements for structural integrity, safety and resilience. It is important to note that structural health monitoring (SHM) represents an interesting solution for the management of these structures, especially today as the industry of sensors and acquisition and transmission systems continues to progress in furtherance to the data processing and analysis techniques and numerical simulation tools that are continually improving (Farrar and Worden 2007). Current research in SHM essentially aims at taking advantage of the benefits described above with a view to developing processes that can extract the maximum useful information on structural characteristics that are sensitive to various types of damages, at the lowest possible cost, while completing the qualitative synthesis and subjectivity of the human element (Brownjohn 2007, Phares *et al*. 2004).

Furthermore, a large number of studies have focused on the identification of structural damages and thus the structural integrity assessment. In this respect, different classification schemes have been used. The majority of methods currently available fall into two basic categories: dynamic and static methods. The first category is based on the examination of modal characteristics that are extracted from vibration testing data (Fan and Qiao 2011, Avci *et al*. 2021), while the second one is generally based on the static responses of strain and displacement, (Bakhtiari-Nejad *et al*. 2005, Terlaje and Truman 2007, Abdo 2012, Seyedpoor and Yazdanpanah 2014, OBrien *et al*. 2015, Boumechra 2017, Grandić and Grandić 2017, Le *et al*. 2019, Lee and Eun 2019, Yazdanpanah *et al*. 2020). It should be noted that the static and dynamic methods can be subdivided into model-based methods and data-based methods (Barthorpe 2010). In the first case, a numerical reference model in finite elements of the healthy (undamaged) structure is

*Corresponding author, Ph.D. Student,
E-mail: iglouli.sidali@gmail.com
[a] Professor, E-mail: n_boumechra@yahoo.fr
[b] Professor, E-mail: karim@unipv.it

ISSN: 1738-1584 (Print), 1738-1991 (Online)

continuously updated through the resolution of an inverse problem using algorithms based on linear algebra and on the optimization theory. This therefore makes it possible to identify the damages using the measurement data collected on the test structure (Friswell 2007). Furthermore, for data-based methods, statistical models and machine learning or pattern recognition algorithms can be used to classify the different characteristics that are extracted from the system measurement data into various damage classes (Sohn *et al*. 2001). Additionally, one can distinguish between the local approaches that aim to provide information about a specific region of a structural element, and the global methods that use a network of sensors to provide global information about the condition of the structure (Chen 2018). The performance of any SHM system depends on the level of accessibility to the information collected on the damage (its detection, location, extent, and estimation of the residual life of the structure under study) (Rytter 1993).

It is worth indicating that despite the significant amount of research work conducted on bridge structural damage detection systems which investigated numerical models or small-scale experimental models in the laboratory, relatively little work has been conducted in-situ on real structures (Ko and Ni 2005, Brownjohn *et al*. 2011, Nagarajaiah and Erazo 2016, Moughty and Casas 2017, An *et al*. 2019, Sun *et al*. 2020). It should be acknowledged that damage is not easy to cause voluntarily on real bridges because they are expensive, besides this is not legally authorized. However, numerical models and laboratory models can be used for that purpose. Additionally, no one denies the facility of control testing in the lab than on an actual bridge (Bao *et al*. 2012, Wang *et al*. 2013, An *et al*. 2013, 2014, Lee *et al*. 2014, Fan *et al*. 2016, Yu and Zhu 2017, Blachowski *et al*. 2017, Liu and Zhang 2018, Zhang and Liu 2019).

In particular, steel truss bridges have been the subject of several contributions in the literature. In some works, (Chang and Kim 2016, Goi and Kim 2017, Kim *et al*. 2016), the authors performed dynamic tests on two steel truss bridges in Japan by subjecting them to artificial damage. Data were recorded for different loading situations and for a large number of sensor configurations. Subsequently, several statistical patterns of damage-sensitive features were investigated for the purpose of detecting pre-applied damages. Some other researchers, Behmanesh and Moaveni (2015), Mustafa *et al*. (2015), Mustafa and Matsumoto (2017), developed probabilistic approaches that are based on the Bayesian scheme to detect and locate the simulated damages on the Dowling Hall Footbridge, the Saraighat Bridge, and on another truss bridge. These approaches were based on updating the numerical model using the modal parameters that were extracted from the recorded acceleration responses. It was found that the success of these methods depends primarily on the accuracy of the initial finite element model, the selected update parameters, on the residuals under consideration and on their weights. By applying the temporal moment approach to the acceleration recordings, Svendsen *et al*. (2020, 2022), were able to detect and locate faulty (defective) connections on the Hell bridge test arena. They also created an unsupervised learning system that allows identifying damages on the same bridge using only experimental data (local/global responses). Regarding Nuno (2013), he used the curvature of the frequency response function (FRF) to analyze the data collected on the steel bridge over the Göta Älv River (Sweden). It was found that, under certain conditions, the approach could successfully detect and locate pre-applied damages. As for Chen *et al*. (2015), they proposed a new technique based on stress influence lines to locate damages. This approach was then validated through a case study that was conducted on the deck of the Tsing Ma suspension bridge in Japan. Nguyen *et al*. (2020), used the transmissibility function, calculated from measured vibration responses under train and ambient excitations, combined with machine learning algorithms and artificial neural network to detect, locate and estimate the damage level on the Nam O railway truss bridge in Vietnam.

The present work focuses mainly on a recently developed method (Boumechra 2017), that is based on an inverse analysis of the static displacement responses of a structure subjected to a moving load. This with the aim of finding the real stiffness and detecting a possible change in stiffness through a comparison with a numerical reference model developed in finite elements and representing the healthy structure. The numerical results obtained for the studied truss bridge showed that the adopted approach allows detecting, localizing and successfully quantifying the reductions or changes in the pre-applied stiffnesses. By applying the same principle to the stress and displacement data for a reduced model of a steel bridge deck developed in the laboratory, the inverse analysis allowed the detection of additional rigidities that were attributed to some surface elements that were omitted in the initial numerical model (Iglouli *et al*. 2018). It is useful to recall that the purpose of this work consists in applying the developed method to a real bridge. The structure under consideration is a truss skew railway bridge located in Ouled Mimoun (Tlemcen, Algeria). This bridge is an excellent example for our study because it suffered from various impacts, mainly from trucks, causing significant damage to its central part. The normal stresses due to the passage of a real train were calculated from recorded strains using strain gauges placed on certain elements of the bridge. Based on the estimated responses, an inverse analysis was developed based on the numerical model of the structure in order to detect damaged areas and to assess the damage rate as well.

2. Experimental investigation

2.1 Description of the structure

Many railway development plans and projects have been implemented in Algeria since the second half of the 19th century. In the northwestern part of the country, the Western Algerian Railways Company built the railway section between Tabia and Tlemcen (64 km) in 1889 on the railway line linking Oued Tlelat to Tlemcen as part of the second extension plan. This railway section had 11 metal (wrought

Fig. 1 General view of the bridge of Ouled Mimoun (Tlemcen - Algeria)

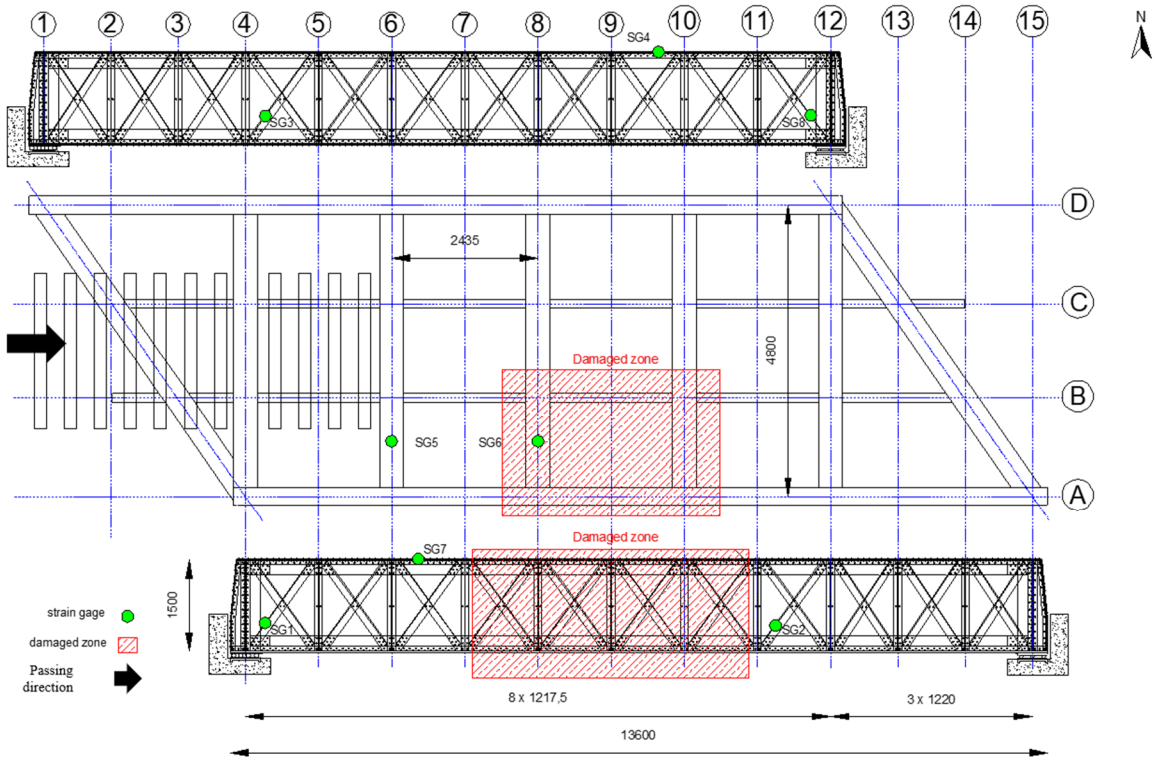

(a) Damaged areas and position of strain Agauges

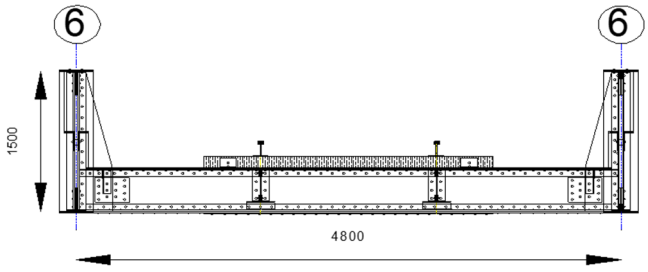

(b) Cross section

Fig. 2 Plan and elevation view of the bridge

iron) bridges. As shown in Fig. 1, the structure in question is a skew metal bridge, located at the entrance to the railway station of Ouled Mimoun. The structure is composed of two main truss girders, measuring 13.6 m in length and 1.50 m in height, and a lower 4.80 m wide deck. This deck is crossed by a single unballasted railway track that is supported by wooden sleepers directly laid on the stringers, as is clearly shown in Figs. 2(a)-(b). The bridge simply rests on two abutments made of cut stone masonry. The elements of the bridge are made from wrought iron sheets and angles, assembled with rivets. Physical and mechanical tests on wrought iron samples were carried out in the laboratory and gave the following results: density = 7.3; E = 1785.108 kN/m^2; fy = 245 N/mm^2; A = 14.4% (Boumechra and Hamdaoui 2008, Boukezzi *et al*. 2021).

(a) Out-of-plane plastic deformation

(b) Damaged central area

(c) Plastic deformation of the diagonal

(d) Tearing of a diagonal

(e) Concentrated plastic deformations

(f) Detachment of deck plates

Fig. 3 Pathologies identified on the structure

2.2 Pathological record of the structure

During its 130 years of service, the bridge has been subjected to several impacts from trucks, particularly during the last few decades, due to its low elevation above the road (3.6 m). This caused multiple damages to its central part, between the axes 7 and 11, as it is explicitly depicted in Fig. 2(a). As for Fig. 3(a), it shows that, among the pathologies noted on the bridge, there is an out-of-plane plastic deformation on the central part of the main beam on the southern side. Likewise, Fig. 3(b) shows that part of the lower chord of the beam is plasticized, and even partially torn across its width. In addition, a strong local plastic deformation and some partial fractures appear on the vertical and diagonal members of the panels (5-7, i.e., axes 8-11), as shown in Figs. 3(b)-(d). Furthermore, according to Fig. 3(e), some plastic deformations and separate cracks were concentrated on the lower flanges of the bridge floor beams and the stringers in the central part, i.e., axes 6-10. Moreover, Fig. 3(f) shows the detachment of the decking in the impacted area (axis 8). In addition, corrosion was observed, with varying degrees, on all the elements, but it was particularly noticeable on the area affected by the impact, on the southern side.

It is worth emphasizing that, although the bridge is damaged, it is still operational. This observation pushed us to carry out an in-depth study for the evaluation of the damage rate in the elements of the bridge. For this, we applied a mathematical method of inverse analysis based on the responses recorded by a set of strain gauges when a train passed over the bridge.

2.3 Experimental procedure

The bridge was tested during the months of December and January of the year 2019. For this, eight strain gauges were placed on certain elements of the bridge as shown in Fig. 2(a). The choice of their location was based on the selection of elements that presented numerically significant stresses as well as on the elements closest to the damaged area. This choice was also conditioned by the accessibility to the measurement points. The strain responses due to the passage of different trains were recorded as well.

Furthermore, strain measurements were carried out using the HBM linear strain gauges (LY11-10/120) which were mounted in a five-wire half-bridge circuit: one strain gauge in the longitudinal direction of the element, a compensation strain gauge on a separate steel part, not loaded and subjected to the same temperature conditions, as shown in Figs. 4(a)-(b). This configuration allows

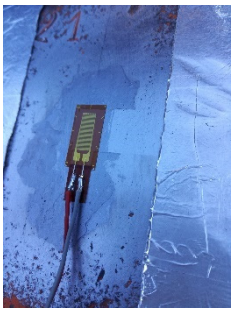

(a) Longitudinal strain gauge

(b) Compensation strain gauge

(c) Data acquisition system

Fig. 4 Experimental strain measurement

Fig. 5 View of the train travelling along the railway bridge

Table 1 Information about the train travelling along the railway bridge

Parameter	Train 1	Train 2
Time of train passage	10:52	16:49
Train speed	10.97 m/s	7.75 m/s
Number of axles	18	18
Weight (locomotive axle)	18.22 T	18.22 T
Weight (passenger car axle)	10 T	10 T
Strain gauge concerned	SG1, SG2, SG3, SG4	SG5, SG6, SG7, SG8

increasing the signal sensitivity and at the same time compensating for the adverse effects of long connection cables (voltage drop, zero drift) as well as for those of temperature variations. This configuration also helps to counterbalance the effects of temperature variations on the cables and the element. A carrier frequency power supply of 4.8 kHz along with a shielded and properly grounded cabling was used for the purpose of reducing or eliminating the electromagnetic noise and thermoelectric voltages, as recommended by the manufacturer HBM (Hoffmann 2012, Keil 2017). It should also be noted that the data acquisition, which is displayed in Fig. 4(c), was performed using the HBM Quantum MX410 amplifier, with a sampling frequency that was chosen to be 50 Hz. The visualization and processing of the computing data were carried out using the Catman software (HBM). In addition, a battery and a voltage converter were provided for powering the equipment used.

The rest of the study is based on the data recorded by the eight strain gauges shown in Fig. 2(a) as the passenger train crosses the bridge, as shown in Figs. 5 and 6. This train is composed of a General Motors GT 22 CW locomotive and three passenger cars. Table 1 and Fig. 6 give more details about the train running on the bridge as well as the scheme used for the loads. Fig. 7 presents the normal stress responses calculated from recorded strains over time with respect to the position of the moving load. It is easy to observe the effect of the passage of the moving load of each group of axles. The curves in this figure exhibit a symmetrical behaviour around the considered sections: they increase, as the force gets closer and then start decreasing as they move away from the examined section. The magnitude of stresses changes considerably between the different components.

Table 2 summarizes the extreme values induced by the passage of the locomotive axles as well as those of the

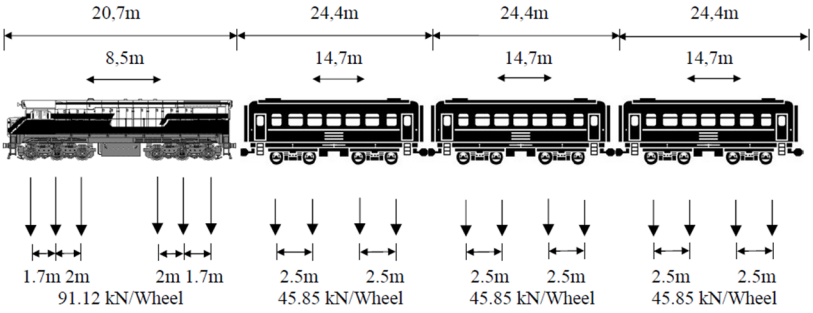

Fig. 6 Configuration of the train travelling along the railway bridge

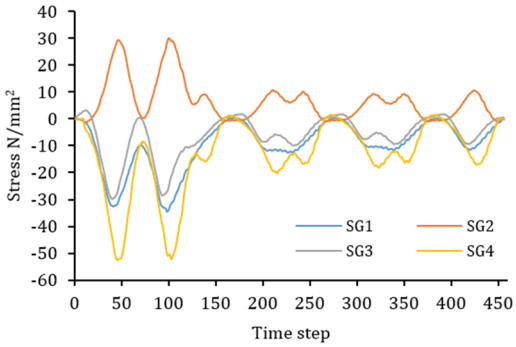

(a) Stresses under train 1

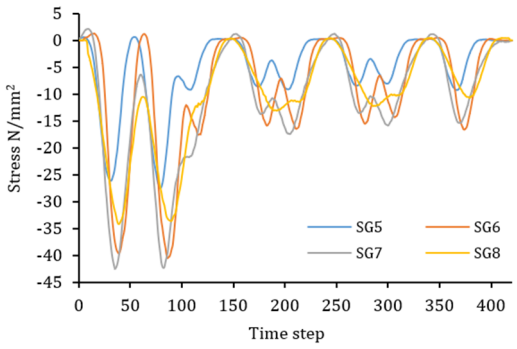

(b) Stresses under train 2

Fig. 7 Normal stress responses estimated from strain gauges SG1 - SG8

Table 2 Maximum estimated stresses

Element of the bridge	Maximum stress under locomotive axles (N/mm²)	Maximum stress under passenger car axles (N/mm²)
(SG1) Diagonal on south side 2	-34.9	-12.8
(SG2) Diagonal on south side 1	30.9	11.3
(SG3) Diagonal on north side 1	-29.9	-9.7
(SG4) North side upper chord	-53.2	-20.7
(SG5) Bridge floor beam 1	-27.6	-9.3
(SG6) Bridge floor beam 2	-40.6	-16.6
(SG7) South side upper chord	-42.5	-17.1
(SG8) Diagonal on north side 2	-34.3	-13.3

passenger wagons. One may easily see that the dynamic component of the responses is negligible. These responses are quasi-static because firstly the train moves through the bridge with a quite low speed (speed of train1 = 39.5 km/h, speed of train 2 = 27.9 km/h) and secondly the bridge has a high structural rigidity.

Furthermore, it should be noted that a maximum value of -53 N/mm² was estimated on the compression chord of the northern side girder (SG4). However, a value of 42.5 N/mm² was estimated on the compression chord on the southern side near the damaged zone (SG7). Moreover, on axis 6 (SG5), the upper fiber of the bridge floor beam experiences maximum compressive stresses equal to -27.6 N/mm², while that located in the damaged area (axis 8 - SG6) showed higher values, (i.e., -40.6 and -16.6 N/mm²), under the locomotive axle load and the passenger wagon axle load, respectively. Considering the operating mode, it was difficult to place a strain gauges on the bottom chord of the girders.

3. Inverse analysis

3.1 Mathematical development

In this work, a numerical method based on an inverse analysis of the static responses of a bridge subjected to a moving load is used Boumechra (2017). The main idea is to determine the real stiffness of a bridge structure crossed by a real train using the normal stress responses calculated from recorded strains using strain gauges. The real global stiffness matrix is defined as

$$K = K_0 + \sum_{i=1}^{n} \alpha_i . K_i \tag{1}$$

Where $\boldsymbol{K}_0$ and $\boldsymbol{K}_i$ are, respectively, the global and elementary stiffness matrices of the healthy structure. n is the number of finite elements constituting the FE model of the bridge. These matrices are obtained from the geometric data, the mechanical characteristics of the materials, and the support conditions. To each rigidity $\boldsymbol{K}_i$ of the finite element i is associated a correction coefficient α_i that defines the possible change in its rigidity. This coefficient may correspond to damage if α_i is negative or to a rigidity excess if it is positive. This correction coefficient is assumed to be the same for the axial, bending, and torsional stiffnesses of the finite element. Developing the static equilibrium equation of the system for each location of the train (x_0) allows writing

$$K\delta(x_0) = f(x_0) \quad \Rightarrow \quad \delta(x_0) = K^{-1} f(x_0) \tag{2}$$

Where $\mathbf{f}(x_0)$ and $\boldsymbol{\delta}(x_0)$ are respectively, the global force and displacement vectors of the system. Due to the large size of the system, it was decided to use the Neumann series to inverse the global stiffness matrix

$$\begin{aligned} K^{-1} &= \left(K_0 + \sum_{i=1}^{n} \alpha_i K_i \right)^{-1} \\ &= \sum_{q=0}^{t} \left(-K_0^{-1} \sum_{i=1}^{n} \alpha_i K_i \right)^{q} K_0^{-1} \end{aligned} \tag{3}$$

Substituting Eq. (3) into Eq. (2), the equilibrium equation becomes

$$\delta(x_0) = \sum_{q=0}^{t}\left(-K_0^{-1}\sum_{i=1}^{n}\alpha_i K_i\right)^q K_0^{-1} f(x_0) \quad (4)$$

From the global displacement vector $\boldsymbol{\delta}(x_0)$, relatively to train location (x_0), the local displacement vector $\boldsymbol{\delta}_{L,j}(x_0)$ of the examined finite element j is determined using the known matrix relation

$$\delta_{L,j}(x_0) = T_{r,j} L_{L,j} \delta(x_0) \quad (5)$$

Where $T_{r,j}$ and $N_{L,j}$ are respectively, the rotation and the identification matrices. The examined finite elements j correspond to the bridge elements on which strain gages are placed.

Thus, the local force vector of the finite element j could be presented as

$$f_{L,j}(x_0) = K_{L,j}\,\delta_{L,j}(x_0) = \left(K_{L,0,j} + \alpha_j\, K_{L,0,j}\right)\delta_{L,j}(x_0) \quad (6)$$

Here, K_L, $K_{L,0}$ are respectively, the real local stiffness and the assumed healthy local stiffness matrices.

Substituting Eqs. (4) and (5) into Eq. (6) also, gives

$$f_{L,j}(x_0) = K_{L,j} T_{r,j} N_{L,j} \sum_{q=0}^{t}\left(-K_0{}^{-1}\sum_{i=1}^{n}\alpha_i K_i\right)^q K_0{}^{-1} f(x_0) \quad (7)$$

On the other hand, for a frame finite element j, defined by its extreme nodes 1 and 2, this local force vector is represented by

$$f_{L,j}(x_0) = \left[N_1, V_{y1}, V_{z1}, M_{x1}, M_{y1}, M_{z1}, N_2, V_{y2}, V_{z2}, \ldots \right.$$
$$\left. M_{x2}, M_{y2}, M_{z2}\right]^T \quad (8)$$

The corresponding normal stress on a section S of the frame finite element j, at a point defined by its local coordinates x_L, y_L and z_L, is defined by

$$\sigma_{j,s}(x_0) = \frac{N}{A} + \frac{M_y}{I_y} z_L + \frac{M_Z}{I_Z} y_L \quad (9)$$

The substitution of Eq. (7) into Eq. (9) allows obtaining a polynomial equation with n variables α_i, and with degree T (order of the Neumann series). Displacing the moving load (train) through the bridge (m positions for example) creates m force vectors ($\mathbf{f}_k = \mathbf{f}(x_0)$; $x_0 = k.\,\Delta L$; $k = 1, m$). It should be noted that calculating m stress values from the corresponding recorded strains, using M strain gauges, placed on some selected elements j ($j = 1, M$), makes it possible to develop a system of ($\varepsilon = j.k = M.m$) nonlinear equations with n unknowns α_i. The problem then becomes a system of $m.M$ polynomial equations and n unknowns.

$$f\left(\alpha_{i=1,n}\right)_{\varepsilon=1,M.n} = \left\{\sigma_{s,exp,\varepsilon} - \sigma_{s,\varepsilon}(\alpha_i)\right\}_{\varepsilon=1,M.n} \quad (10)$$

Furthermore, the Levenberg-Marquardt optimization algorithm is used to solve the system mentioned above and represented by Eq. (10). This mathematical development is used to write a code called the Inverse Analysis Finite Element Method (IAFEM) under the Matlab software in order to perform the inverse analysis of the stress responses that are estimated from recorded strains on the real structure using a finite element model of the healthy structure, and to determine the correction coefficients α_i. From these results, damages or changes in the structure of the bridge may be detected.

3.2 Numerical reference model

Several simulations were carried out using the Sap2000 software in order to better understand the behaviour of the bridge and to define an adequate numerical model that can represent the structure under study for the purpose of applying the method previously developed. For this, two models were elaborated: a frame finite element model and a shell finite element model, as shown in Fig. 8. Different comparisons are presented in the following sections.

3.2.1 Frame and shell finite element numerical models

The shell finite element numerical simulation converges towards normal stress values that are relatively close to those of the frame finite element model. A difference, not exceeding 5%, was recorded on tensile diagonals and compressive diagonals, as is clearly shown in Figs. 9(a)-(b).

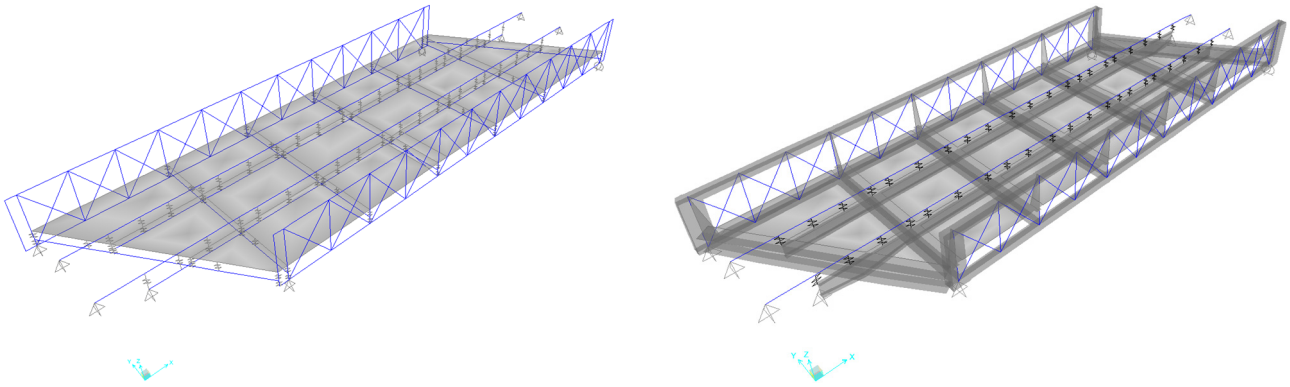

(a) Frame element (b) Shell element

Fig. 8 Finite element model - SAP2000

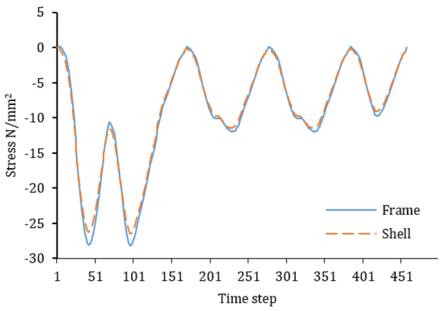

(a) Diagonal Member stress – Compression

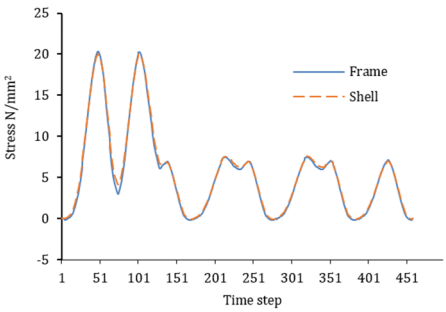

(b) Diagonal Member stress -Tension

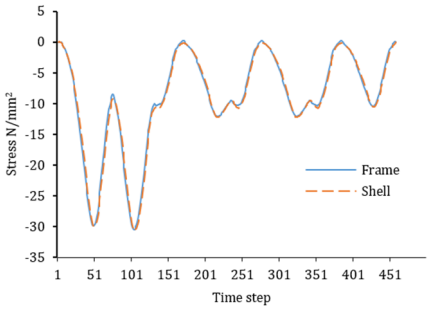

(c) Top Chord stress

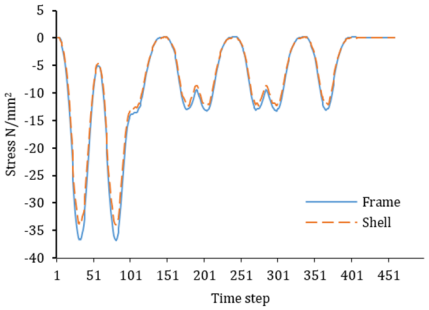

(d) Floor beam stress

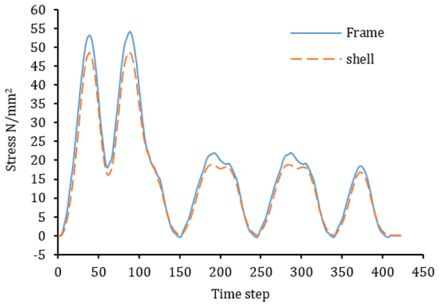

(e) Bottom Chord stress

Fig. 9 Comparison of finite element normal stresses between a frame element and a shell element

However, Fig. 9(c) indicates that this difference is between 1 and 2% when comparing the top chords of the main girders. Regarding Fig. 9(d), it shows that this deviation varies from 1 to 5% for the bridge floor beams in the central zone. A maximum difference of 8% was observed and shown in Fig. 9(e) for the bottom chord, which is the most stressed.

3.2.2 Influence of metal decking

Several simulations were carried out with and without the flooring of the deck in order to better understand the effect of the surface elements on the behaviour of the different components of the bridge. Figs. 10(a)-(c) explicitly shows that the effect of the metal decking on the normal stress behaviour of the diagonals and the top chord of main girders is negligible. Indeed, the difference does not

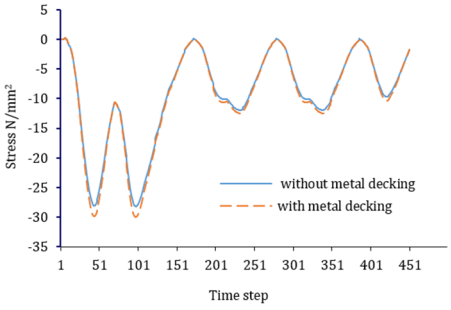

(a) Diagonal Member stress – Compression

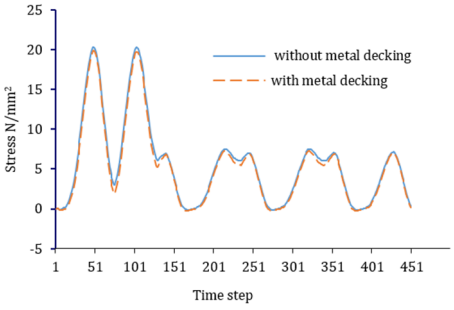

(b) Diagonal Member stress – Tension

Fig. 10 Finite Element normal stresses – Metal decking effect

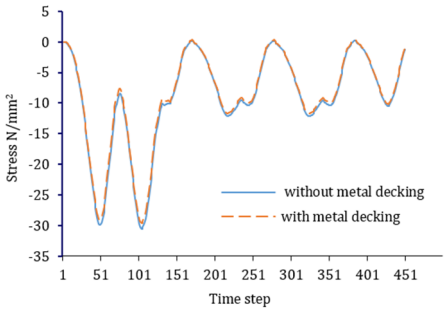

(c) Top Chord stress

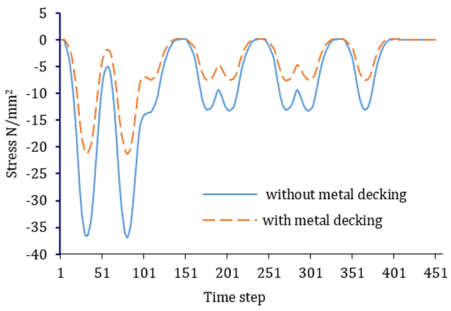

(d) Floor beam stress

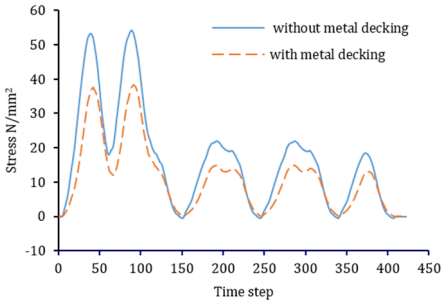

(e) Bottom Chord stress

Fig. 10 Finite Element normal stresses – Metal decking effect

exceed 5%. However, the bridge floor beams have a significant effect; the difference can reach 75%, as is clearly depicted in Fig. 10(d). This observation is quite obvious because in the presence of the metal deck plate, the stiffness of the deck increases. In fact, a part of the applied forces is absorbed by the deck, which engenders a drop in the normal stress value. A similar effect was also observed on the bottom chord of the main girders (see Fig. 10). In this case, the difference is estimated at 45%.

3.2.3 Comparison of experimental and numerical stress responses

Figs. 11(a)-(h) illustrates the superposition of the experimental signals, which were calculated from recorded strains on the damaged bridge, and the numerical ones in the frame element of the bridge in the healthy state. A simple comparison between the stress signals estimated from the strain gauges data and the digital signals of the healthy bridge shows a difference between -10 and -15% on the compressed diagonals (SG1, SG3 and SG8), while a greater deviation of +26% was observed on the damaged side of the bridge on the tension diagonal (SG2). The difference was found to exceed -40% on the bridge floor beam (SG5 – axis 6), whereas this difference of only +1% was recorded on the bridge floor beam located in the damaged zone (SG6 – axis 8). Similarly, a deviation of +30% was observed on the upper chord of the main girder on the northern side (SG4), and another one of +13% on that of the damaged southern side.

Considering the results of the previous numerical simulations, it was decided to make some simplifications to the reference model. The numerical model retained for the inverse analysis was constructed using the 3D frame element, which contains 6 degrees of freedom per node, as indicated in Fig. 12. The bridge support conditions were taken into account in accordance with the reality. In addition, rigid links were assigned to the connection points (stringers-bridge floor beams) and (bridge floor beams-main beams) in order to take into account the offset between the centres of gravity of the sections of the

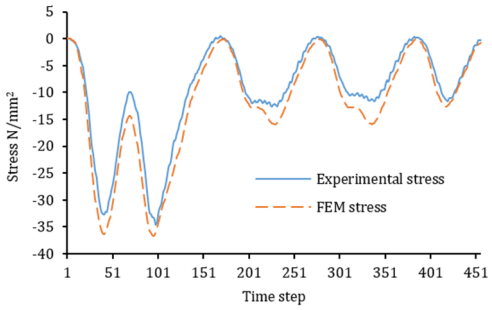

(a) Diagonal Member stress – Compression

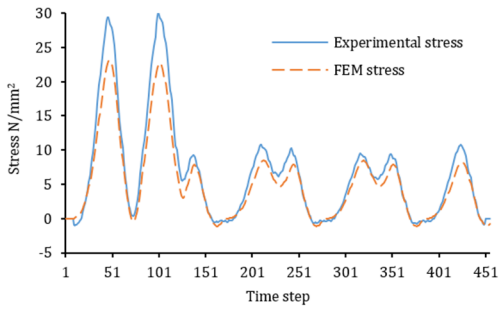

(b) Diagonal Member stress – Tension

Fig. 11 Experimental and numerical stress responses

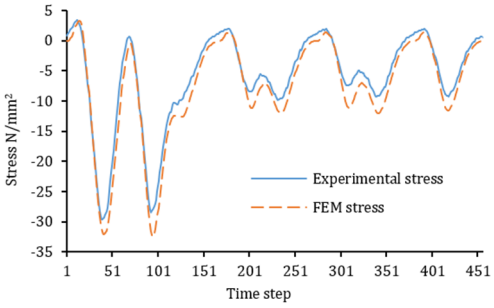

(c) Top Chord stress

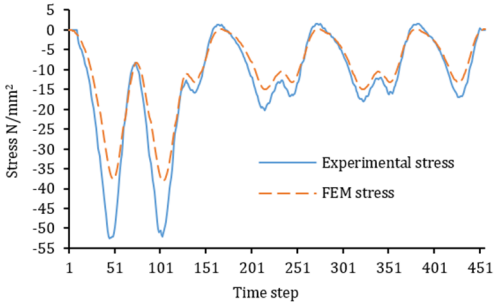

(d) Floor beam stress

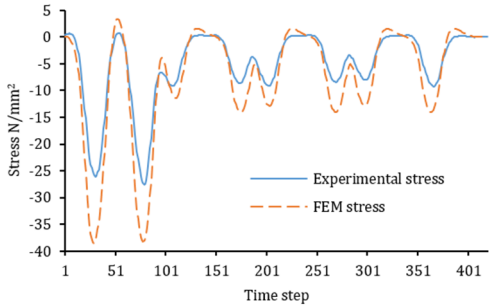

(e) Signal (SG5) Floor beam

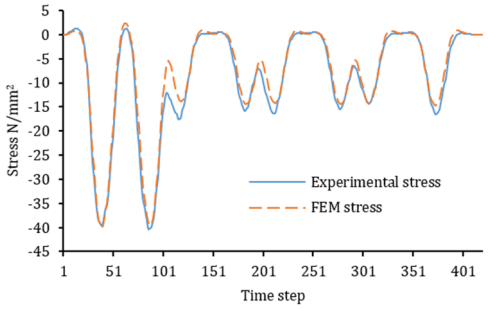

(f) Signal (SG6) Floor beam

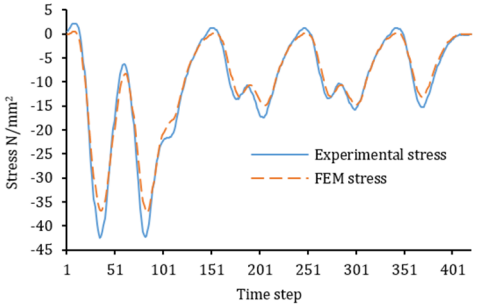

(g) Signal (SG7) Top Chord

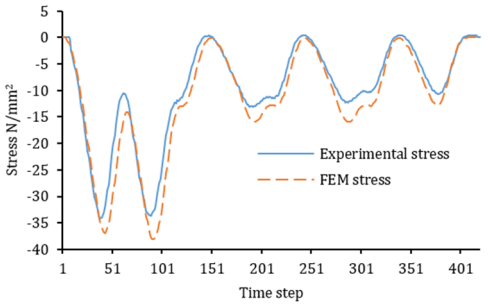

(h) Signal (SG 8) Diagonal Memberr

Fig. 11 Experimental and numerical stress responses

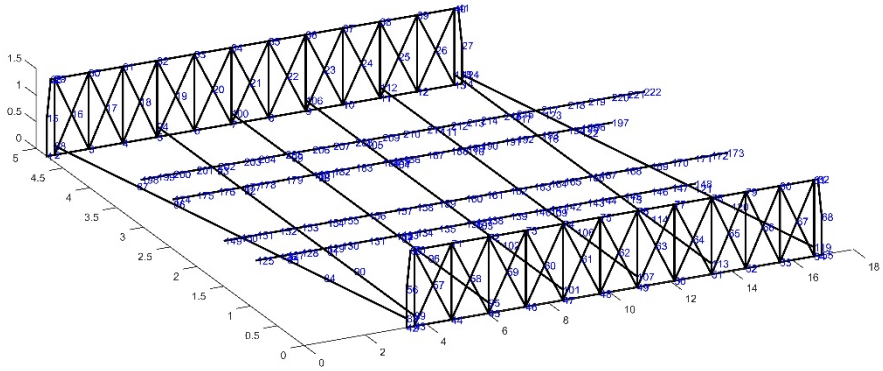

Fig. 12 Reference finite element model using MATLAB

assembled elements. It should be noted that the transmission of loads between the rail and the deck is ensured by simple connections that are applied to the contact points under the wooden sleepers. In order to reduce the number of the unknowns, and the time of inverse analysis, the surface elements (gussets and floor of the deck) are neglected.

A calculation code was developed using the Matlab software in order to carry out a static analysis of the bridge that is subjected to a real moving train. The first part of the code allows developing the different numerical components of Eq. (7). (i.e., the global stiffness matrix of the healthy bridge, the stiffness matrices of the different finite elements of the bridge components taken separately, the force vectors

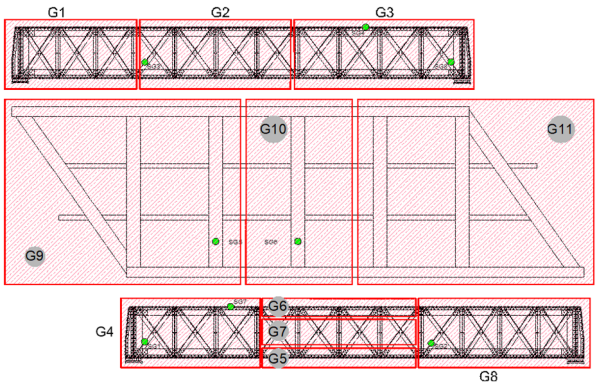

Fig. 13 Identification of groups of elements

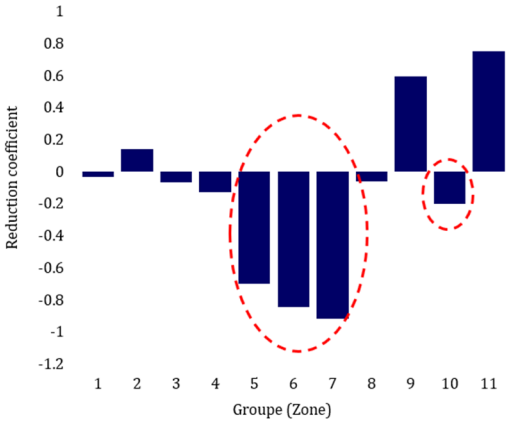

Fig. 14 Reduction coefficients corresponding to each group of elements G1 - G11

Table 3 Input data of the inverse analysis

Designation	Value
Number of estimated stress responses (points examined)	8
Number of finite element groups (Number of unknowns)	11
Number of equations (data)	3648
Order of Neumann series	12
Accuracy on objective function	1.10^{-6}
Accuracy of the solution (Levenberg-Marquardt)	1.10^{-6}

of the train at each position x_0 as it travels on the bridge and the geometric characteristics of checked elements). The second part of the code processes the strain gauge responses and solves Eq. (10) using the Levenberg-Marquardt optimization method.

4. Results and discussion

The inverse analysis of the experimental responses using the algorithm that is based on the inverse finite element method (IFEM) was initially carried out on a bridge model that was discretized in 301 finite elements; each component of the bridge represents a finite element. In this variant, the algorithm was not successful in locating the elements that are really damaged because the number of responses used was insufficient compared to the number of unknowns in the system (301 unknowns for 3648 data). Hence, it was decided to adopt a different approach. The structure was then decomposed into groups of finite elements, defined by regions, in order to reduce the number of unknowns in the system to be solved. Fig. 13 gives a schematization of the group identification. The elements belonging to the same group were assigned to the same stiffness correction coefficient. The number of unknowns is reduced to 11. Table 3 summarizes the input data.

As indicated in Fig. 14, the inverse analysis results gave positive correction coefficients, varying from 0.03 to 0.14, in regions 1, 2, and 3 which correspond to the main girder on the north side; this element is not damaged. Furthermore, negative coefficients were observed in zones 4, 5, 6, 7, and 8that correspond to the beam elements on the south side; these elements were affected by the impact. The negative coefficients are higher in the central part, with a maximum value of -0.91. Table 4 presents the different results and

Table 4 Damage rate and pathologies observed

Region	Damage rate/ stiffness excess (%)	Observation made on the damaged bridge
G1	-0.1	Healthy region
G2	+13.8	
G3	-7.5	
G4	-12.8	- Out-of-plane deformation - Plastic ball joints - Ruptures in the diagonals and lower chord of the southern side beam - Detachment of rivets
G5	-70.9	
G6	-83.2	
G7	-89	
G8	-8.7	
G9	+58.4	Healthy region with extra rigidity (metal plating)
G10	+20.4	Detachment of the flooring and plastic deformations concentrated on the lower chord of the bridge floor beams and stringers
G11	+83.8	Healthy zone with extra rigidity (metal decking)

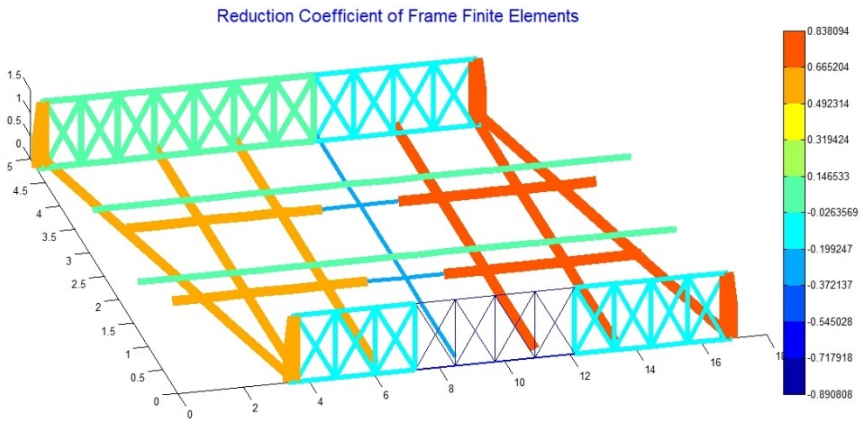

Fig. 15 3D graphical representation of the reduction coefficient of the structure components

their significance in terms of the pathologies observed on the bridge. In addition, a 3D graphical representation of the damage rates of the different structural components is shown in Fig. 15.

Moreover, the findings confirm the damage previously observed, i.e., the out-of-plane deformation of the girder on the southern side, between the axes (7 and 11), the tears on its bottom chord, and the local buckling on the diagonals, as illustrated in Figs. 3(a)-(d).

Except for the central part (zone 10) which shows a stiffness reduction of -20%, the rest of the deck (zones 9 and 11) shows positive correction coefficients, with a rate greater than +60%. The stiffness reduction is due to the plastic deformations that are concentrated on the bridge floor beams and on the stringers of the central part as well as to the detachment of the flooring, as is clearly depicted in Figs. 3(e)-(f).

The positive coefficients of zones 9 and 11 confirm the presence of additional stiffness on the deck elements. These additional rigidities are due to the metal decking initially that was neglected in the numerical reference model. This result explains well the discrepancy between the experimental and digital signals that were recorded by strain gauge 5 (see Fig. 11(e)). As for Fig. 10(d), it confirms the effect of the metal decking.

It can also be clearly seen that the detachment of the decking in the central bridge part caused the stiffness to decrease, which resulted in a behaviour similar to that given by the numerical reference model, as illustrated in Fig. 11(f).

It is interesting to note that despite the low rigidity remaining on the central part elements of the south side lateral beam (11 to 29% compared to the healthy state), the bridge still resists and it is operational. This can be explained by the overdimensioning of the whole bridge elements in addition to the system's high degree of hyperstaticity and thus, its impact on the stresses redistribution.

5. Conclusions

This study focused on an old wrought iron railway bridge, dating from the 19th century. The bridge suffered from damages in the bottom chord of the girder. An inverse analysis was carried out on the normal stress responses, which were calculated from recorded strains by a set of eight strain gauges, placed in well-chosen positions on the bridge. The strains were recorded during the passage of a passenger train using an experimental device. The characteristics (position and weight of axles) of the train are known. The purpose of this work is to check the performance of the numerical method for the localization and quantification of the damage rate on the real bridge.

It turned out that the frame finite element model was the most appropriate because we are dealing with a truss bridge. Considering the design adopted for the bridge, one could note the absence of the dynamic component on the recorded signals, which facilitated the use of the numerical method.

It should also be emphasized that applying the previously developed code is greedy in data because the number of unknowns is quite important. It was therefore necessary to reduce the number of unknowns in groups of finite elements that correspond to distinct parts of the bridge. It turned out that the inverse analysis results converge well, and give concordant and very interesting results.

The findings of the study made it possible to successfully locate the damaged zones of the metal bridge, and also to make a correct estimate of the damage rate and stiffness excess in other areas. Moreover, it was possible to detect the presence of rigidity of the surface elements, which were not taken into account in the reference numerical model.

It is also important to note that a larger number of sensors (strain gages) at several other locations, under various operational conditions, could provide more information on the behaviour of the damaged bridge and thus improve the accuaracy on the positions and rates of damages.

The method developed in this work offers to engineers an efficient tool that allows the analysis of structures (railway bridges or road bridges) that are constantly subjected to moving loads, and to detect possible damages to these structures. This method represents a cost-effective solution for monitoring the health of bridges.

The application of the inverse analysis on continuous strain data (through a network of sensors placed on the

elements of the bridge), makes it possible to continuously update the real stiffness of the structural elements with respect to a numerical reference model, representing the healthy bridge. This makes it possible to design a smart structural health control system to detect, locate damaged elements and thus quantify the rate of damage in real time. An automatic alert triggering system can also be integrated to warn owners, limit risks and facilitate decision-making.

References

Abdo, M.A.B. (2012), "Parametric study of using only static response in structural damage detection", *Eng. Struct.*, **34**, 124-31. https://doi.org/10.1016/j.engstruct.2011.09.027

An, Y., Li, B. and Ou, J. (2013), "An algorithm for damage localization in steel truss structures: numerical simulation and experimental validation", *J. Intell. Mater. Syst. Struct.*, **24**(14), 1683-1698. https://doi.org/10.1177/1045389x13483027

An, Y., Ou, J.P., Li, J. and Spencer, B.F. (2014), "Stochastic DLV method for steel truss structures: simulation and experiment", *Smart Struct. Syst.*, *Int. J.*, **14**(2), 105-128. https://doi.org/10.12989/sss.2014.14.2.105

An, Y., Chatzi, E., Sim, S.H., Laflamme, S., Blachowski, B. and Ou, J. (2019), "Recent progress and future trends on damage identification methods for bridge structures", *Struct. Control Health Monit.*, **26**(10). https://doi.org/10.1002/stc.2416

Avci, O., Abdeljaber, O., Kiranyaz, S., Hussein, M., Gabbouj, M. and Inman, D.J. (2021), "A review of vibration-based damage detection in civil structures: from traditional methods to machine learning and deep learning applications", *Mech. Syst. Signal Process.*, **147**. https://doi.org/10.1016/j.ymssp.2020.107077

Bakhtiari-Nejad, F., Rahai, A. and Esfandiari, A. (2005), "A structural damage detection method using static noisy data", *Eng. Struct.*, **27**, 1784-1793. https://doi.org/10.1016/j.engstruct.2005.04.019

Bao, Y., Li, H., An, Y. and Ou, J. (2012), "Dempster-Shafer evidence theory approach to structural damage detection", *Struct. Health Monitor.*, **11**(1), 13-26. https://doi.org/10.1177/1475921710395813

Barthorpe, R.J. (2010), "On model and data based approaches to structural health monitoring", Ph.D. Dissertation; University of Sheffield, UK.

Behmanesh, I. and Moaveni, B. (2015), "Probabilistic identification of simulated damage on the dowling hall footbridge through bayesian finite element model updating", *Struct. Control Health Monitor.*, **22**(3), 463-483. https://doi.org/10.1002/stc.1684

Blachowski, B., An, Y., Spencer, B.F. and Ou, J. (2017), "Axial strain accelerations approach for damage localization in statically determinate truss structures", *Comput.-Aided Civil Infrastruct. Eng.*, **32**(4), 304-318. https://doi.org/10.1111/mice.12258

Boukezzi, L., Benaissa, A., Lehbab-Boukezzi, Z. and Nasser, B. (2021), "Assessment of existing steel railway bridges, algeria", *Eur. J. Environ. Civil Eng*, **25**(1), 117-131. https://doi.org/10.1080/19648189.2018.1518792

Boumechra, N. (2017), "Damage detection in beam and truss structures by the inverse analysis of the static response due to moving loads", *Struct. Control Health Monit.*, **24**(10). https://doi.org/10.1002/stc.1972

Boumechra, N. and Hamdaoui, K. (2008), "Dynamic and Fatigue Analysis of an 18th Century Steel Arch Bridge", *AIP Conference Proceedings 1020* (PART 1), Calabria, July.

Brownjohn, J.M. (2007), "Structural health monitoring of civil infrastructure", *Phil. Trans. R. Soc. A*, **365**(1851), 589-622. https://doi.org/10.1098/rsta.2006.1925

Brownjohn, J.M., De Stefano, A., Xu, Y.L., Wenzel, H. and Aktan, A.E. (2011), "Vibration-based monitoring of civil infrastructure: challenges and successes", *J. Civil Struct. Health Monitor.*, **1**(3-4), 79-95. https://doi.org/10.1007/s13349-011-0009-5

Chang, K.C. and Kim, C.W. (2016), "Modal-parameter identification and vibration-based damage detection of a damaged steel truss bridge", *Eng. Struct.*, **122**(2), 156-173. https://doi.org/10.1016/j.engstruct.2016.04.057

Chen, H.P. (2018), *Structural Health Monitoring of Large Civil Engineering Structures*, Wiley-Blackwell, London, UK.

Chen, Z.W., Zhu, S., Xu, Y.L., Li, Q. and Cai, Q.L. (2015), "Damage detection in long suspension bridges using stress influence lines", *J. Bridge Eng.*, **20**(3), 5014013. https://doi.org/10.1061/(asce)be.1943-5592.0000681

Fan, W. and Qiao, P. (2011), "Vibration-based damage identification methods: a review and comparative study", *Struct. Health Monitor.*, **10**(1), 83-111. https://doi.org/10.1177/1475921710365419

Fan, X., Li, J. and Hao, H. (2016), "Piezoelectric impedance based damage detection in truss bridges based on time frequency ARMA model", *Smart Struct. Syst.*, *Int. J.*, **18**(3), 501-523. https://doi.org/10.12989/sss.2016.18.3.501

Farrar, C.R. and Worden, K. (2007), "An introduction to structural health monitoring", *Phil. Trans. R. Soc. A*, **365**(1851), 303-315. https://doi.org/10.1098/rsta.2006.1928

Friswell, M.I. (2007), "Damage identification using inverse methods", *Phil. Trans. R. Soc. A*, **365**(1851), 393-410. https://doi.org/10.1098/rsta.2006.1930

Goi, Y. and Kim, C.W. (2017), "Damage detection of a truss bridge utilizing a damage indicator from multivariate autoregressive model", *J. Civil Struct. Health Monitor.*, **7**(2), 153-162. https://doi.org/10.1007/s13349-017-0222-y

Grandić, I.Š. and Grandić, D. (2017), "Estimation of damage severity using sparse static measurement", *J. Civil Eng. Manage*, **23**(2), 213-221. https://doi.org/10.3846/13923730.2015.1027256

Hoffmann, K. (2012), *An Introduction to Stress Analysis and Transducer Design Using Strain Gauges*.

Iglouli, S., Boumechra, N. and Hamdaoui, K. (2018), "Damage or change detection in a small scale model of steel bridge deck under static loading by extensometery", *Iop Conference Series: Materials Science and Engineering*, Prague, September.

Keil, S. (2017), *Technology and Practical Use of Strain Gages*, (1st edition), Ernst & Sohn, Germany.

Kim, C.W., Chang, K.C., Kitauchi, S. and McGetrick, P.J. (2016), "A field experiment on a steel gerber-truss bridge for damage detection utilizing vehicle-induced vibrations", *Struct. Health Monitor.*, **15**(2), 174-192. https://doi.org/10.1177/1475921715627506

Ko, J.M. and Ni, Y.Q. (2005), "Technology developments in structural health monitoring of large-scale bridges", *Eng. Struct.*, **27**, 1715-1725. https://doi.org/10.1016/j.engstruct.2005.02.021

Le, N.T., Thambiratnam, D.P., Nguyen, A. and Chan, T.H.T. (2019), "A new method for locating and quantifying damage in beams from static deflection changes", *Eng. Struct.*, **180**, 779-792. https://doi.org/10.1016/j.engstruct.2018.11.071

Lee, E.T. and Eun, H.C. (2019), "Disassembling-based structural damage detection using static measurement data", *Shock Vib.*, 2019. https://doi.org/10.1155/2019/6073828

Lee, S.G., Yun, G., Rahimi, M.R. and Shang, S. (2014), "Experimental validation of multistep quantitative crack damage assessment for truss structures by finite element model updating", *Smart Mater. Struct.*, **23**(12). https://doi.org/10.1088/0964-1726/23/12/125034

Liu, Y. and Zhang, S. (2018), "Damage localization of beam bridges using quasi-static strain influence lines based on the botda technique", *Sensors*, **18**(12). https://doi.org/10.3390/s18124446

Moughty, J.J. and Casas, J.R. (2017), "A state of the art review of modal-based damage detection in bridges: development, challenges, and solutions", *Appl. Sci.*, **7**(5). https://doi.org/10.3390/app7050510

Mustafa, S. and Matsumoto, Y. (2017), "Bayesian model updating and its limitations for detecting local damage of an existing truss bridge", *J. Bridge Eng.*, **22**(7), 4017019. https://doi.org/10.1061/(asce)be.1943-5592.0001044

Mustafa, S., Debnath, N. and Dutta, A. (2015), "Bayesian probabilistic approach for model updating and damage detection for a large truss bridge", *Int. J. Steel Struct.*, **15**(2), 473-485. https://doi.org/10.1007/s13296-015-6016-3

Nagarajaiah, S. and Erazo, K. (2016), "Structural monitoring and identification of civil infrastructure in the united states", *Struct. Monitor. Maint., Int. J.*, **3**(1), 51-69. https://doi.org/10.12989/smm.2016.3.1.051

Nguyen, D.H., Tran-Ngoc, H., Bui-Tien, T., De Roeck, G. and Wahab, M.A. (2020), "Damage detection in truss bridges using transmissibility and machine learning algorithm: Application to Nam O bridge", *Smart Struct. Syst., Int. J.*, **26**(1), 35-47. https://doi.org/10.12989/sss.2020.26.1.035

Nuno, K. (2013), "Damage detection of a steel truss bridge using frequency response function curvature method", KTH Royal Institute of Technology, TRITA-BKN Rapport.

Obrien, E., Carey, C. and Keenahan, J. (2015), "Bridge damage detection using ambient traffic and moving force identification", *Struct. Control Health Monitor.*, **22**(12), 1396-1407. https://doi.org/10.1002/stc.1749

Phares, B.M., Washer, G.A., Rolander, D.D., Graybeal, B.A. and Moore, M. (2004), "Routine highway bridge inspection condition documentation accuracy and reliability", *J. Bridge Eng.*, **9**(4), 403-413. https://doi.org/10.1061/(asce)1084-0702(2004)9:4(403)

Rytter, A. (1993), "Vibrational based inspection of civil engineering structures", Ph.D. Dissertation; University of Alborg, Denmark.

Seyedpoor, S.M. and Yazdanpanah, O. (2014), "An efficient indicator for structural damage localization using the change of strain energy based on static noisy data", *Appl. Mathe. Modell.*, **38**(9-10), 2661-2672. https://doi.org/10.1016/j.apm.2013.10.072

Sohn, H., Farrar, C.R., Hunter, N.F. and Worden, K. (2001), "Structural health monitoring using statistical pattern recognition techniques", *J. Dyn. Syst. Meas. Control*, **123**(4), 706-711. https://doi.org/10.1115/1.1410933

Sun, L., Shang, Z., Xia, Y., Bhowmick, S., Nagarajaiah, S. (2020), "Review of bridge structural health monitoring aided by big data and artificial intelligence: from condition assessment to damage detection", *J. Struct. Eng.*, **146**(5), 4020073. https://doi.org/10.1061/(asce)st.1943-541x.0002535

Svendsen, B.T., Frøseth, G.T. and Rönnquist, A. (2020), "Damage detection applied to a full-scale steel bridge using temporal moments", *Shock Vib.*, 1-16. https://doi.org/10.1155/2020/3083752

Svendsen, B.T., Frøseth, G.T., Øiseth, O. and Rønnquist, A. (2022), "A data-based structural health monitoring approach for damage detection in steel bridges using experimental data", *J. Civil Struct. Health Monit.*, **12**(1), 101-115. https://doi.org/10.1007/s13349-021-00530-8

Terlaje, A.S. and Truman, K.Z. (2007), "Parameter identification and damage detection using structural optimization and static response data", *Adv. Struct. Eng.*, **10**(6), 607-621. https://doi.org/10.1260/136943307783571409

Wang, F.L., Chan, T.H.T., Thambiratnam, D.P. and Tan, A.C.C. (2013), "Damage diagnosis for complex steel truss bridges using multi-layer genetic algorithm", *J. Civil Struct. Health Monitor.*, **3**(2), 117-127. https://doi.org/10.1007/s13349-013-0041-8

Yazdanpanah, O., Izadifard, R.A. and Dehestani, M. (2020), "Static data based damage localization of beam-column structures considering axial load", *Mech. Adv. Mater. Struct.*, **27**(16), 1433-1450. https://doi.org/10.1080/15376494.2018.1513612

Yu, L. and Zhu, J.H. (2017), "Structural damage prognosis on truss bridges with end connector bolts", *J. Eng. Mech.*, **143**(3). https://doi.org/10.1061/(asce)em.1943-7889.0001052

Zhang, S. and Liu, Y. (2019), "Damage detection in beam bridges using quasi-static displacement influence lines", *Appl. Sci.*, **9**(9), 1805. https://doi.org/10.3390/app9091805

FC